Front. Earth Sci. 2017, 11(2): 385–396
DOI 10.1007/s11707-016-0586-z

RESEARCH ARTICLE

Geomorphic change in Dingzi Bay, East China since the 1950s: impacts of human activity and fluvial input

Qing TIAN (✉)[1], Qing WANG[2], Yalong LIU[3]

1 Oceanic Modeling and Observation Laboratory, School of Marine Science, Nanjing University of Information Science and Technology, Nanjing 210044, China
2 Coast Institute, Ludong University, Yantai 264025, China
3 Yantai Marine Environmental Monitoring Center Station, State Oceanic Administration, Yantai 264000, China

Abstract This study examines the geomorphic evolution of Dingzi Bay, East China in response to human activity and variations in fluvial input since the 1950s. The analysis is based on data from multiple mathematical methods, along with information obtained from Remote Sensing, Geographic Information System and Global Position System technology. The results show that the annual runoff and sediment load discharged into Dingzi Bay display significant decreasing trends overall, and marked downward steps were observed in 1966 and 1980. Around 60%–80% of the decline is attributed to decreasing precipitation in the Wulong River Basin. The landform types in Dingzi Bay have changed significantly since the 1950s, especially over the period between 1981 and 1995. Large areas of tidal flats, swamp, salt fields, and paddy fields have been reclaimed, and aquaculture ponds have been constructed. Consequently, the patterns of erosion and deposition in the bay have changed substantially. Despite a reduction in sediment input of 65.68% after 1966, low rates of sediment deposition continued in the bay. However, deposition rates changed significantly after 1981 owing to large-scale development in the bay, with a net depositional area approximately 10 times larger than that during 1961–1981. This geomorphic evolution stabilized following the termination of large-scale human activity in the bay after 1995. Overall, Dingzi Bay has shown a tendency towards silting-up during 1952–2010, with the bay head migrating seaward, the number of channels in the tidal creek system decreasing, and the tidal inlet becoming narrower and shorter. In conclusion, large-scale development and human activity in Dingzi Bay have controlled the geomorphic evolution of the bay since the 1950s.

Received September 10, 2015; accepted February 14, 2016

E-mail: tianqing0405@hotmail.com

Keywords sediment load, runoff, human activity, geomorphic evolution, Dingzi Bay

1 Introduction

Estuarine and coastal zones are facing great threats on a global scale due to factors such as coastline retreat, decreasing delta progradation rates, delta erosion, and decreasing fluvial discharge and sediment input (Xu, 2001; Frihy et al., 2003; Chu et al., 2006; Yang et al., 2011; Kong et al., 2015a, b). Fluvial systems are the main sources of continental sediment discharged into marine basins; however, many of the river systems worldwide have been experiencing declining water and sediment loads since the 1950s, mainly as a result of climate change and human activity in the drainage basin (e.g., reservoir and dam construction, land cover changes, soil and water conservation measures, and water diversions) (Walling, 2006; Oudin et al., 2008; Miao et al., 2010; Wang et al., 2010; Xu et al., 2010; Harish et al., 2012; Wu et al., 2012; Dai and Liu, 2013). In addition, estuarine and coastal zones have undergone large-scale exploitation. For instance, aquaculture ponds are common in coastal zones and have been constructed on large scales in recent decades, driven by economic interests (Xie and Yu, 2007; Ramos e Silva et al., 2010). Consequently, hydrodynamic and morphodynamic conditions in estuarine and coastal areas have frequently been strongly modified, thereby affecting the ecological environment and functioning of these areas. As a result, estuarine and coastal areas have become particularly fragile and liable to instability when subjected to external influences (Xie et al., 2004; Yang et al., 2005, 2006, 2011; Syvitski and Saito, 2007; Lu and Chen, 2008; Dai et al., 2011, 2013a).

The geomorphic responses of large bays and estuaries to decreasing fluvial inputs and human activity have been reported worldwide (Chu et al., 2006; Yang et al., 2011; Dai et al., 2013b; Kong et al., 2015a). Previous studies have mainly focused on large bays dominated by large mature rivers, whilst small bays have received less research focus. However, small bays not only outnumber large bays globally, but are more sensitive to human disturbance and environmental change (Eric et al., 1999; Farnsworth and Milliman, 2003). Milliman and Syvitski (1992) suggested that the effects of sediment transport from small mountainous rivers on geomorphic features in estuarine and coastal areas have been underestimated. Consequently, research data derived from small bays are of great importance for understanding the evolution of coastal zones, and will provide a theoretical basis for sustainable management and the ecological restoration in coastal areas.

This study examines the geomorphic evolution of Dingzi Bay in the southern Jiaodong Peninsula, East China (Fig. 1), by analyzing the combined effects of fluvial flux variations and human activity since the 1950s. Dingzi Bay is located along a bedrock coast in a mountainous region with a temperate climate and formed during the Holocene marine transgression following the last glacial epoch (Xia and Liu, 1990; Wang, 1993). The present-day features of Dingzi Bay comprise a main tidal channel and large areas of intertidal mudflats. The wide intertidal zone has important impacts on the hydrodynamic conditions (e.g., tides, waves, and runoff) in the bay, and variations in these conditions will lead to changes in geomorphic features (Prandle, 2003; Brown and Davies, 2010). In contrast to large bays which have extensive areas of open water, Dingzi Bay is a relatively small and shallow semi-enclosed bay, resulting in weak hydrodynamic conditions. Dingzi Bay is predominantly fed by a small mountainous river, the Wulong River (Fig. 1), which has a drainage basin of ~2652 km^2 (Sun et al., 1987). Because this area is dominated by the East Asian Summer Monsoon, more than 70% of the annual rainfall, runoff, and sediment load in the Wulong River Basin occur during the wet season (June–September) (Shandong Provincial Department of Land and

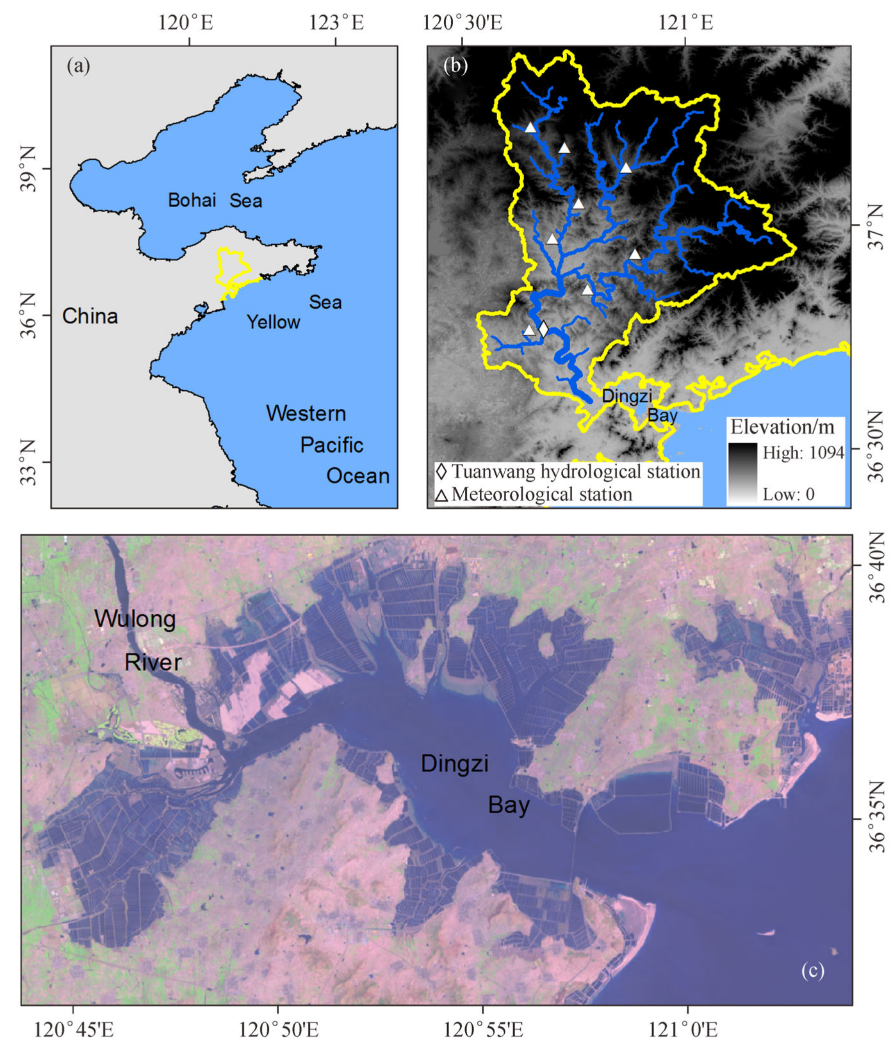

Fig. 1 Sketch map of Dingzi Bay.

Resources China, 2007).

There are many other bays with similar characteristics in the southern Jiaodong Peninsula, including Jinghai, Wuleidao, and Rushan bays. However, Dingzi Bay is the largest and considered the most representative for the purpose of this study. Most of the small bays in the southern Jiaodong Peninsula have not been studied. Therefore, this research is of great value in further understanding the geomorphic features of small bays and their development in similar settings to those of the present study.

2 Data and methodology

2.1 Data

Data were collated from measured annual runoff and sediment load data from the Tuanwang hydrological station in the Wulong River estuary (Fig. 1(b)) to discern any temporal changes in fluvial flux into Dingzi Bay. The spatially averaged values of measured annual precipitation obtained from eight meteorological stations were used to assess changes in climate in the Wulong River Basin since the 1950s (Fig. 1(b)).

Changes in the geomorphic features and landforms of Dingzi Bay were assessed from topographic maps, nautical charts, and remote sensing images obtained in 1961, 1981, 1995, and 2010. There is only one nautical chart available for the study area in the 1960s. This chart only covers part of Dingzi Bay (area B as shown in Fig. 2), and it was surveyed in 1961. The topographic map of Dianji surveyed during the 1960s was used to reconstruct the landform distributions in areas A and C in 1961, as no major changes in landforms were observed during this time. This means that the landform data for Dingzi Bay in 1961 were compiled from two sources (Fig. 2). The landform data for 1981 are based on the topographic map of Wangcun, as surveyed in 1981. The landform data for 1995 and 2010 were derived from remote sensing images (Table 1).

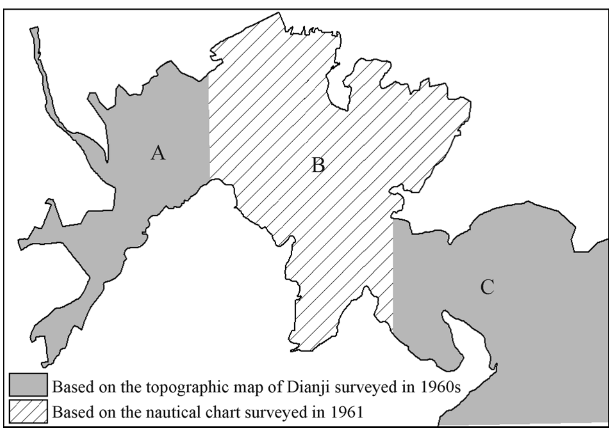

Fig. 2 Landform data source of Dingzi Bay in 1961.

Among the images, those captured during periods with the lowest tide were selected for use in this study.

2.2 Methodology

2.2.1 The non-parametric Mann-Kendall test

The non-parametric Mann-Kendall test (MK test) was first used to describe the monotonic change trend of the hydro-meteorological time-series. This test is based on the null hypothesis Ho, which supposes that the analyzed time-series are independent and randomly ordered, and there is no obvious change trend (e.g., Xu et al., 2010; Wu et al., 2012), and it contains two parameters: Zc and β.

Zc reflects the general change trend of the series. For the analyzed series ($x_1, x_2, \ldots, x_n$)

$$Zc = \begin{cases} \dfrac{S-1}{\sqrt{\mathrm{var}(S)}} & S > 0 \\ 0 & S = 0\,, \\ \dfrac{S+1}{\sqrt{\mathrm{var}(S)}} & S < 0 \end{cases} \tag{1}$$

$$S = \sum_{i=1}^{n-1} \sum_{j=i+1}^{n} sign(x_j - x_i), \tag{2}$$

$$sign(x_j - x_i) = \begin{cases} 1 & x_j - x_i > 0 \\ 0 & x_j - x_i = 0\,, \\ -1 & x_j - x_i < 0 \end{cases} \tag{3}$$

$$\mathrm{var}(S) = \frac{n(n-1)(2n+5)}{18}. \tag{4}$$

α is the significance level for the test, $\pm Z_{1-\alpha/2}$ are the standard normal deviates. Zc follows the standard normal distribution. Therefore, Ho will be rejected if $|Zc| \leqslant Z_{1-\alpha/2}$ (abbreviated as R), which means there is a significant change trend for the series, while accepting H_0 (abbreviated as A) suggests no obvious trend. Besides, $Zc > 0$ represents an upward trend, a negative trend conversely. $\alpha = 95\%$ was applied in this paper, $\pm Z_{1-\alpha/2} = \pm 1.96$.

β provides an estimation of the average change rate of the series. It is based on the assumption that the change trend of the series is monotonic.

$$\beta = Median\left(\frac{x_i - x_j}{i - j}\right) \qquad (1<j<i<n). \tag{5}$$

But it should be noted that the observed series may be autocorrelated in many real situations, and will lead to misinterpretation of the Mann-Kendall test result. Therefore, a modified Mann-Kendall test (MMK) (Hamed and Rao, 1998) which removed the effect of autocorrelation

Table 1 List of remote sensing images used in the present study

Image	Type	Acquisition time	Resolution/m	Tidal level/m
LE71200352000340SGS00	TM	2000-12-05-02-26-28	30	0.08
LE71190352000061SGS00	TM	2000-03-01-02-22:37	30	– 0.07
LE71200352000068EDC00	TM	2000-03-08-02-28:44	30	– 1.04
LE71200352000020EDC00	TM	2000-01-20-2-28:43-10	30	– 1.44
LT51200351995254XXX01	TM	1995-09-11-01-38:06-32	30	– 0.88
LE71200352010319EDC01	ETM +	2010-11-08-02-22:23-50	30	– 0.30

was also used in this study. If the p-value of the test is less than the significance level, Ho is rejected; otherwise, there is insufficient evidence to reject Ho.

2.2.2 Accumulated anomaly curve

The periodical fluctuation of the time-series was analyzed by drawing an Accumulated Anomaly Curve (e.g., Tian et al., 2016). The accumulated anomaly of every point was given as:

$$X_t = \sum_{i=1}^{t}(X_i - \overline{X}) \qquad (t = 1,2,...,n), \tag{6}$$

$$\overline{X} = \frac{1}{n}\sum_{i=1}^{n} X_i. \tag{7}$$

The rising limb of the curve can be interpreted to indicate a flood period relative to the runoff series. Conversely, the falling limb of the curve can be interpreted to represent a relative drought period.

2.2.3 Order cluster analysis

The exact transition point was detected by Order Cluster Analysis (OCA). This statistical method is used to find the optimal dividing point of a time-series without disrupting the sequence of the series (e.g., Li et al., 2003). The time-series $(x_1,...x_i...x_j...x_n)$ $(1 < i < j < \text{n})$ with n points was divided into m groups, then the point with the minimum $\varphi\{p\ (m,\ n)\}$ value is the optimal dividing point:

$$\{i_1, i_1 + 1 = 2,...,i_2 - 1\}\{i_2, i_2 + 1,...,i_3 - 1\}...$$
$$\{i_k, i_k + 1,...,i_{k+1} - 1\}\{i_m, i_m + 1,...,n\}$$

$$D(i,j) = \sum_{k=i}^{j}\left(x_k - \overline{x}_{ij}\right)'\left(x_k - \overline{x}_{ij}\right), \tag{8}$$

$$\overline{x}_{ij} = \frac{1}{j - i + 1}\sum_{k=i}^{j} x_k, \tag{9}$$

$$\varphi\{p(m,n)\} = \sum_{k=1}^{m} D(i_k, i_{k+1} - 1). \tag{10}$$

2.2.4 Multiple linear regression equation

Multiple linear regression equations were derived to separate the climatic and anthropogenic impacts on the fluvial inputs into Dingzi Bay (e.g., Hao et al., 2008). Assuming that hydrological variables (Y; e.g., runoff and sediment load) were primarily related to climatic conditions and little impacted by human activity in the early part of the study period, a multiple linear regression equation can be constructed where X is natural influencing factors (e.g., precipitation):

$$Y = mX_1 + nX_2 + c. \tag{11}$$

In which, m, n and c are constant terms. Measured X values were used to predict the estimated Y values (which were assumed to not be influenced by human activities) using the equation above. The difference between the estimated Y values before and after the transition points were interpreted to be caused by the climate change. In contrast, the difference between the measured Y values before and after the transition points was attributed to the combined influence of human activity and climate changes. The human impact on the drainage basin could therefore be determined from the variance between these two difference values.

2.2.5 Double mass curve

Plots were created showing cumulative annual runoff against precipitation, and cumulative annual sediment load against runoff. These plots illustrate the influence of human activity on runoff and sediment load in the drainage basin (e.g., Wu et al., 2012).

2.2.6 Identification of landform types

Landform changes in Dingzi Bay were identified from nautical charts, topographic maps, and remote sensing images over the period 1961–2010. All the data were preprocessed before undertaking visual interpretation, including false color synthesis, geometric correction, image fusion and cutting, and strip-removal applied to the ETM + remote sensing image obtained in 2010.

Using Arcgis software, the landform types of Dingzi Bay were divided into two main categories: natural landforms (including tidal flats, water bodies, islands, sand bars, alluvial plain, and hills) and the artificial landforms (including paddy fields, salt fields, and aquaculture ponds). The hills, sand bars, islands, and alluvial plain were excluded from this research because they show minor changes over the study interval.

Taking the mean sea level of the Huanghai Sea as base level, the waterline that separates tidal flats and water bodies on the nautical chart and the topographic map was defined by the lowest level of the local spring tide, with an absolute elevation of –2.04 m. However, the waterlines observed on the remote sensing images were affected by their acquisition time. To counter this issue, a contour line model was built to extract the same waterline with a tidal level of –2.04 m from the remote sensing images. In this study, four remote sensing images in 2000 (Table 1) were used to build the model using the method of Ryu et al. (2008) and Zhao et al. (2008). From these data, the "erosion area" and the "siltation area" were calculated by comparing the waterlines between two periods (e.g., 1961 and 1981). If a tidal flat was transformed into a water body, it was interpreted to have been eroded, whereas if a water body evolved into a tidal flat over time, it was interpreted to have been silted up.

The methodology used in this study leads to uncertainties arising from the subjectivity of the process of obtaining data from visual interpretations. It is suggested that using alternative methods (e.g., Kong et al., 2015a) to extract the waterline in future studies will provide more robust conclusions regarding the geomorphic evolution of Dingzi Bay.

3 Results and discussion

3.1 Temporal changes in runoff and sediment load discharged into Dingzi Bay since the 1950s

The annual precipitation in the Wulong River Basin shows a decreasing trend, but this is not significant at the 95% significance level (original and modified Mann-Kendall test; Table 2). The annual runoff of the Wulong River shows a significant decreasing trend since the 1950s, with an average decreasing rate of ~0.06×10^9 m^3/10yr based on the original MK test (Table 2). The accumulated anomaly curve of annual runoff is similar to that of annual precipitation: an increasing trend was observed for the first 30 years (1952 to the late 1970s), followed by a decreasing trend with a marked change in 1966 (Fig. 3). This indicates that the Wulong River was at a relatively high-flow stage before 1980, followed by a relatively dry or low-flow stage. The year 1980 marks the transition between these stages as detected by OCA, with the annual runoff decreasing by up to 55% after this point (Table 3).

The annual sediment load of the Wulong River shows a significant decreasing trend overall, with an average decrease of 0.17×10^6 t/yr based on the original MK test (Table 2). The accumulated anomaly curve shows an increasing trend to 1965, followed by a period with little change and then a declining trend after 1980, and a

Table 2 Mann-Kendall test results of the hydrological time-series in the Wulong River Basin

Elements	Period	Average value	MK test		MMK test	H_0	Trend [a)]
			Zc	β (/10yr)	p		
Annual precipitation/mm	1952–2009	686.18	−1.81	−24.60	0.07	A	ID
Annual runoff/(10^9 m^3)	1952–2009	0.43	−2.82	−0.06	0.00	R	SD
Annual sediment load/(10^6 t)	1953–2009	0.51	−5.92	−0.17	0.00	R	SD

a) SI: significant increase, II: insignificant increase, SD: significant decrease, ID: insignificant decrease.

Table 3 Transition points in the hydrological time-series for the Wulong River Basin

Elements	OCA	Period	Average value	Variation
Annual precipitation/(mm)	1977	1952–1976	758.36	
		1977–2009	631.49	16.73% [a)]
Annual runoff/(10^9 m^3)	1980	1952–1979	0.60	
		1980–2009	0.27	55.00% [b)]
Annual sediment load/(10^6 t)	1966, 1980	1953–1965	1.46	
		1966–1979	0.50	65.75% [c)]
		1980–2009	0.11	78.00% [d)]

a) 1977−2009 vs 1952−1976, b) 1980−2009 vs 1952−1979, c) 1966−1979 vs 1953−1965, d) 1980−2009 vs 1966−1979.

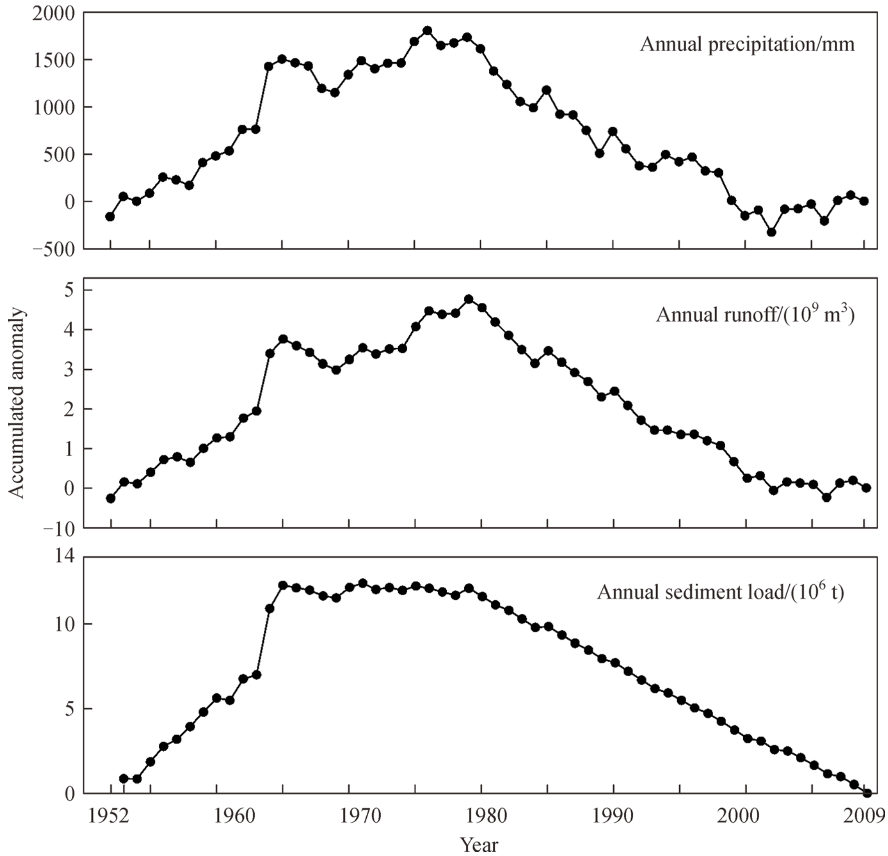

Fig. 3 Accumulated anomaly curves of annual precipitation, annual runoff and annual sediment load of the Wulong River.

horizontal period in between (Fig. 3). This indicates that the annual sediment load was markedly reduced in 1966 and 1980. The annual sediment load decreased by 65.75% after 1966 (by ~0.96×10^6 t) and decreased by 78% after 1980 (Table 3). The reduction in annual runoff and sediment load is greater than the reduction in annual precipitation.

3.2 Separating the climatic and anthropogenic impacts on runoff and sediment load

Precipitation provides the predominant water supply in river basins, particularly in small mountainous rivers with little glacial meltwater input. Since runoff volume controls discharge and the transport capacity of a river, it is the dominant control of fluvial sediment load. Figure 4 shows that the annual fluctuations in runoff and sediment load of the Wulong River are correlated with annual precipitation since the early 1950s. However, runoff and sediment load decreased significantly after 1966 and 1980 due to the combined effects of reduced precipitation and human disturbance in the river basin (Fig. 4).

With the promotion of national agricultural production from the mid-1960s to the 1970s, large areas of farmland on sloping land in the river basins were converted to terraced fields. These land-use changes have led to surface-water runoff retention and reduced rates of soil erosion. Changes in Chinese rural land-use policies have meant that terraced fields were commonly converted to apple orchards after the late 1970s and the early 1980s. At the same time, parts of terraced fields and large areas of grassland were converted to forest, leading to a rapid expansion in areas of orchards and forests since 1980. Numerous studies have shown that sediment loads in rivers flowing through agricultural or uncultivated areas are much higher than loads in rivers flowing through forests or terraced fields (Xu and Sun, 2007; Mohammad and Adam, 2010).

In contrast to large mature rivers that are severely affected by reservoir and dam construction (Li et al., 2011; Yang et al., 2011), the barrages (65 in total) and reservoirs constructed in the late 1950s and 1960s in the Wulong River Basin (Water Resources Department of Shandong Province, 1999) only led to short-term fluctuations in annual runoff and sediment load discharged into Dingzi Bay. The influence of the reservoirs and barrages was likely not significant in the long term (Fig. 5) because of their small scale and location in the upstream tributaries of the river basin. Coarse grains were trapped and removed from the sediment load, whereas the suspended sediment was largely unaffected.

A linear regression equation between annual runoff (R) and annual precipitation (P) of the Wulong River for the

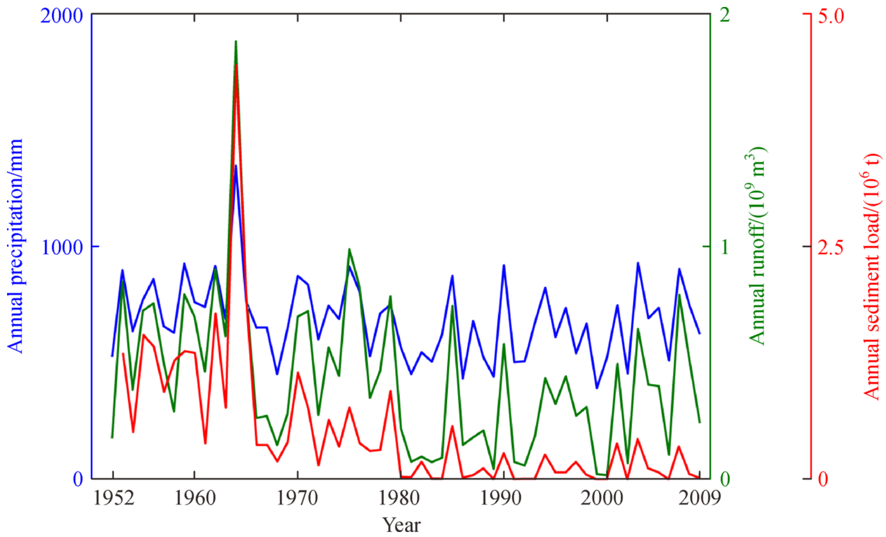

Fig. 4 Time series of annual precipitation, annual runoff, and annual sediment load of the Wulong River.

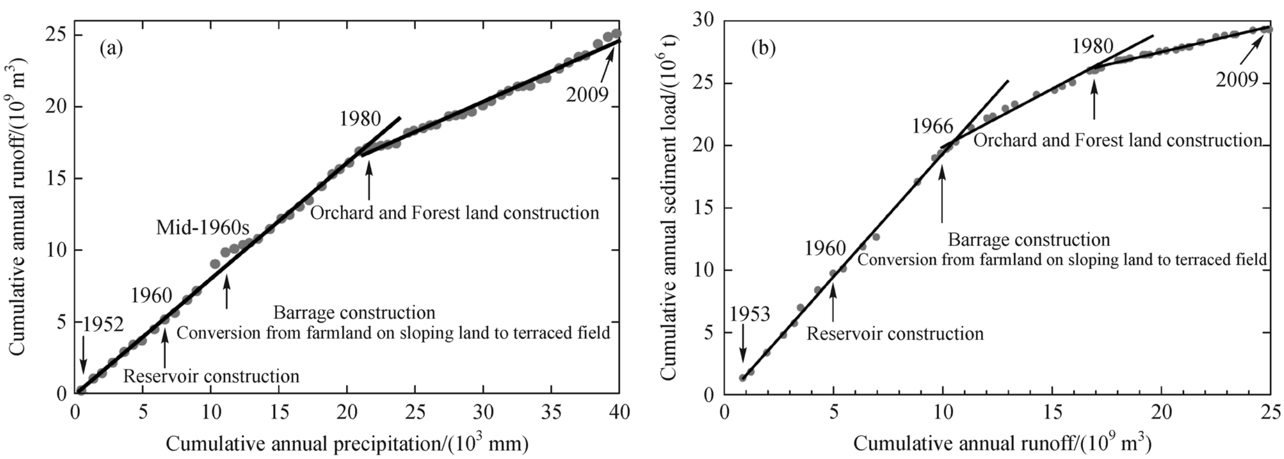

Fig. 5 Plots of cumulative annual runoff against precipitation (a) and plots of cumulative annual sediment load against runoff of the Wulong River (b).

period 1952–1979 was derived as follows:

$$R = 0.02 \times P - 8.4\,(R^2 = 0.91). \quad (12)$$

Estimated values of annual runoff were calculated with observed annual precipitation values using Eq. (12). Figure 5(a) shows that changes in precipitation and human activity (e.g., the establishing of orchards and forests) in the Wulong River Basin accounted for 69.70% and 30.30%, respectively, of runoff reduction after 1980 (Table 4). Table 5 shows that the impact of human activity varies between decades. Sun et al. (2006) reported that afforestation and terrace construction has resulted in a 20%–40% reduction in runoff for the majority of rivers in northern China; this region has also experienced climate warming and water shortages in recent decades.

The multiple linear regression equation between annual runoff (R), precipitation (P), and sediment load (SL) between 1953 and 1965 is as follows:

$$SL = 30.26 \times R - 0.13 \times P + 29.10\,(R^2 = 0.88). \quad (13)$$

Note that the estimated values of sediment load after 1979 were calculated using the estimated values of annual runoff. The reduction in precipitation and runoff resulted in the total sediment load into Dingzi Bay decreasing by 59.38% after 1966, and 76.92% after 1980 (Table 4). The changes in these years significantly influenced the sediment load reduction over the whole study period. The influence and extent of human activity in the river basin became more apparent over time, as indicated by the differences in estimated and observed annual sediment load (Table 5).

Overall, the total amount of water and sediment load discharged into Dingzi Bay from the Wulong River decreased by 60%–80% and 20%–40%, respectively, as a result of changes in precipitation and human activity in the drainage basin since the 1950s. In contrast to major

Table 4 Relative contributions of precipitation change (CP) and human impacts (CH) to the reduction in runoff and sediment load

Elements	Period	Average observed value	Average estimated value	CP	CH
Annual runoff/(10^9 m^3)	1952–1979	0.60	0.60	—	—
	1980–2009	0.27	0.37	69.70% [a)]	30.30% [a)]
Annual sediment load/(10^6 t)	1953–1965	1.46	1.46	—	—
	1966–1979	0.50	0.89	59.38% [b)]	40.62% [b)]
	1980–2009	0.11	0.59	76.92% [c)]	23.08% [c)]

a) 1980–2009 vs 1952–1979, b) 1966–1979 vs 1953–1965, c) 1980–2009 vs 1966–1979.

Table 5 Estimated annual runoff and sediment load during different time periods

Hydrological element	Period	Observed value	Estimated value	Difference value	Influence of human activity
Annual runoff/(10^9 m^3)	1952–1979	16.88	16.88	—	—
	1980–1989	1.87	2.45	0.58	23.67%
	1990–1999	2.69	3.86	1.17	30.31%
	2000–2009	3.67	4.82	1.15	23.86%
Annual sediment load/(10^6 t)	1953–1965	18.98	18.99	—	—
	1966–1979	7.02	12.46	5.44	43.66%
	1980–1989	0.98	2.91	1.93	66.32%
	1990–1999	0.91	6.24	5.33	85.42%
	2000–2009	1.40	8.47	7.07	83.47%

rivers where a reduction in discharge and sediment load is caused mainly by human activity (e.g., Yang et al., 2005; Walling, 2006; Wu et al., 2012), changes in precipitation accounted for the significant reduction of fluvial inputs into Dingzi Bay from the Wulong River Basin.

3.3 Geomorphic evolution of Dingzi Bay since the 1950s

3.3.1 Landform changes in Dingzi Bay

The distribution of landforms in Dingzi Bay has changed significantly since the 1950s (Fig. 6). In 1961, the total area of artificial landforms (primarily salt fields and paddy fields) was 49.14 km^2 and included only small areas of aquaculture ponds. In the same year, the total area of natural landforms (tidal flats, swamps, and water bodies) covered an area of 144.81 km^2, accounting for three-quarters of the total bay area. By 2010 the area of natural landforms had halved, whilst the area of artificial landforms (primarily salt fields and the aquaculture ponds) increased dramatically to 108.4 km^2, or three-fifths of the total bay area (Table 6); paddy fields had almost disappeared. As a result, the increase in area and number of artificial landforms of Dingzi Bay has led to a reduction in the area of natural landforms in recent decades.

The complex changes in landforms in Dingzi Bay between 1961 and 2010 are apparent from the data in Table 7. More specifically, the increases in the area and type of artificial landforms were due mainly to the sharp increase in aquaculture ponds after 1981. Large areas of tidal flats and swamps in the muddy supratidal zone of Dingzi Bay were reclaimed and aquaculture ponds were constructed. Salt fields and paddy fields gradually disappeared because of their lower economic benefits. Large-scale developments and land use changes in Dingzi Bay continued until 1995. At the same time, a northwest–southeast oriented dam was constructed in the north of the bay to prevent intrusions of sea water. Since 1995 the rate of landform change in Dingzi Bay has been relatively slow. Although more aquaculture ponds were constructed during 1995–2010, their numbers were much lower than those constructed during 1981–1995.

In summary, the main landform transformations in Dingzi Bay have included the conversion of tidal flats, swamps, and paddy fields to aquaculture ponds, and the conversion of water bodies to tidal flats (Table 7). These man-made land-use changes were particularly intense during 1981–1995 (Fig. 7).

3.3.2 Changes in accretion and erosion in Dingzi Bay

Prior to 1981, Dingzi Bay was in a natural state and was not significantly affected by human activity. The long and narrow bay has weak hydrodynamic conditions, meaning that a large proportion of the sediment load discharged from the Wulong River is deposited in the bay. The bay has sustained a slow accretion rate despite the sediment input reducing by 65.68% since 1966 (Fig. 8; Table 8). Between

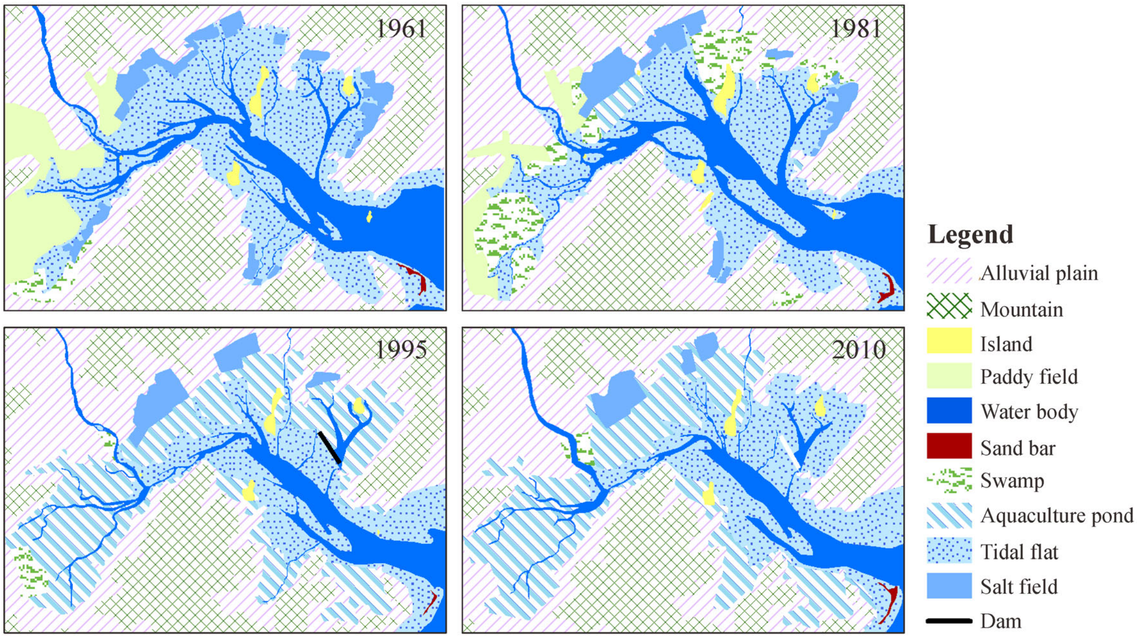

Fig. 6 Distribution of landforms in Dingzi Bay in 1961, 1981, 1995, and 2010.

Table 6 Areas of the main landform types in Dingzi Bay

Year	Artificial landform types/km^2			Natural landform types/km^2		
	Salt field	Paddy field	Aquaculture pond	Tidal flat	Swamp	Water body
1961	14.09	35.05	0	93.04	4.05	47.72
1981	13.80	14.09	3.85	77.51	25.06	46.34
1995	6.74	0	82.99	53.21	4.07	34.66
2010	7.08	0	101.32	42.53	1.85	33.55

Table 7 Transition matrix of landform types in Dingzi Bay during 1961–2010

Landform types	Salt field /km^2	Tidal flat /km^2	Swamp /km^2	Aquaculture pond /km^2	Water body /km^2
Salt field	4.22	6.26	0	3.12	0.06
Tidal flat	2.40	62.05	0.82	21.22	5.01
Swamp	0	0	0	3.79	0.03
Paddy field	0.08	0.88	0.75	16.62	0.42
Water body	0	19.00	0.15	0.53	27.48

1961 and 1981 the land area converted from water bodies to tidal flats was ~1.1 km^2 (Table 8). The volume of sediment deposited in Dingzi Bay could not be calculated in this study because no historical data are available regarding water depth.

The overall conversion from water bodies to tidal flats continued in Dingzi Bay during 1981–1995, but at a much higher rate than that during 1961–1981 (Fig. 8; Table 8). Since the late 1970s and early 1980s, the large-scale construction of aquaculture ponds and dams in tidal flat areas has disconnected the tidal flat from the alluvial plain. This has also changed the landscape and boundary conditions between water bodies and tidal flats, altering the hydrodynamic conditions and leading to rapid accretion in the bay that has continued despite a reduction in sediment load from the Wulong River of 78.09% since 1980. Consequently, the influence of dams and aquaculture ponds construction is much more significant than the influence of reduced fluvial sediment input. Accretion of 11.29 km^2 of sediment has taken place in Dingzi Bay since 1981, which is 10 times greater than the increase during 1961–1981 (Table 8).

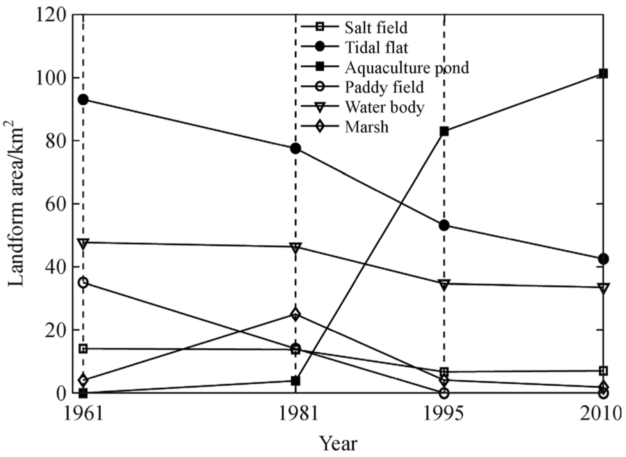

Fig. 7 Landform Changes in Dingzi Bay.

The geomorphic evolution of Dingzi Bay has tended to be stable following the end of large-scale human activity after 1995 (Fig. 8). The complex conversions between water body and tidal flat has significantly decreased, and Dingzi Bay has shown a slight overall erosion since 1995 (Table 8). It can be inferred that erosion in Dingzi Bay will increase in the long term if sediment supply from the Wulong River continues to decline and there is no more large-scale human activity in the bay. Further research is required to clarify the geomorphic evolution in Dingzi Bay, as this will help to prevent ecosystem deterioration and disturbance to marine organisms resulting from the changed geomorphic features and hydrological dynamic conditions (Gao, 1998, 2002).

Human activity has profoundly affected the landform type and distribution in Dingzi Bay since 1981, with a subsequent impact on the pattern of accretion and erosion. In general, the rapid accretion that occurred during 1981–1995 led to degradation of the bay. Figure 6 shows the following overall changes. 1) During 1961–1981 the river delta possessed tidal channels to the north and south. After 1995, the north channel became silted up, resulting in the delta becoming connected to the north shore, whilst the south channel narrowed. Significant deposition in the bay head caused the river mouth to migrate seaward. 2) The main tidal inlet for the bay became shorter and narrower, and the overall area of water bodies showed a marked

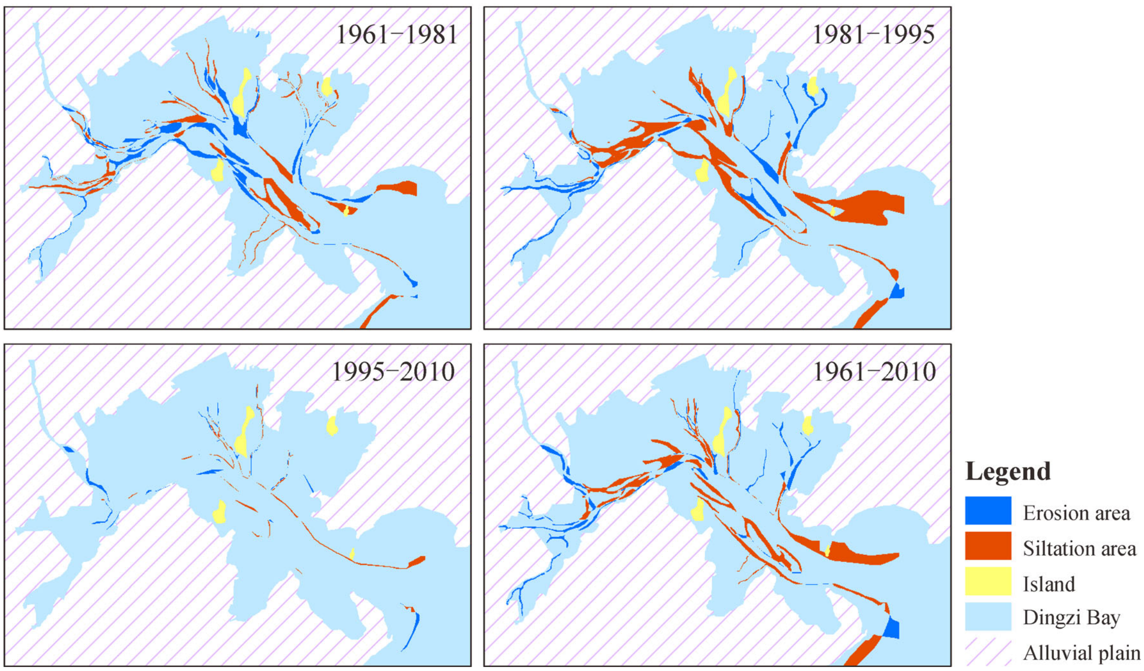

Fig. 8 Spatial distribution of areas of accretion and erosion in Dingzi Bay.

Table 8 Changes in areas of accretion and erosion in Dingzi Bay during 1961–2010

Evolution of accretion and erosion	1961–1981		1981–1995		1995–2010		1961–2010	
	Area/km^2	Rate/(km^2·yr^{-1})	Area/km^2	Rate/(km^2·yr^{-1})	Area/km^2	Rate/(km^2·yr^{-1})	Area/km^2	Rate/(km^2·yr^{-1})
Tidal flat converted to water body	7.77	0.37	6.01	0.4	1.24	0.08	5.02	0.10
Water body converted to tidal flat	8.87	0.42	17.3	1.15	1	0.06	12.96	0.26
Overall conversion	Accretion		Accretion		Erosion		Accretion	

decrease. 3) The original tidal creek system on the tidal flat was destroyed due to the construction of a dam and aquaculture ponds; consequently, the tidal creeks became shorter and narrower.

4 Conclusions

The water and sediment inputs into Dingzi Bay decreased significantly between 1952 and 2009. The years 1966 and 1980 were transition points that resulted from significant changes in precipitation and anthropogenic influences. Decreasing precipitation and the influence of human activity (barrage construction and the rapid expansion of apple orchards and afforestation) in the Wulong River Basin have contributed 60%–80% and 20%–40%, respectively, to the reduction in the total amount of water and sediment load discharged into the bay.

The type and distribution of landforms in Dingzi Bay have changed significantly since the 1950s, particularly between 1981 and 1995. The main landform changed from natural landform types before 1981 to artificial landform types after 1995. These changes were due to reclamation of large areas of tidal flat and swamp to construct aquaculture ponds, and the replacement of salt fields and paddy fields with more profitable aquaculture ponds. Changes in land use have subsequently led to changes in erosion and accretion rates, and their locations within Dingzi Bay. Prior to 1981, human impact in Dingzi Bay was minimal and slow accretion rates were sustainable, given the volume of sediment discharged from the Wulong River. This accretionary behavior was sustained even though sediment inputs into the bay reduced by 65.68% after 1966. Crucially, large-scale tidal flat reclamation and dam construction during 1981–1995 led to an increase in the net siltation area by a factor of ~10 compared with 1961−1981. This dramatic increase in accretion concluded with the termination of large-scale human activity in the bay after 1995. Overall, Dingzi Bay has shown a silting-up trend since the 1950s with progradation of the bay head, a reduction in the number of channels in the tidal creek system, and narrowing and shortening of the main tidal inlet.

In summary, the impacts of large-scale development and human activity in Dingzi Bay after 1981 greatly exceeded those resulting from precipitation changes in the upstream Wulong River Basin. These disturbances have significantly altered the natural geomorphic features and evolution of the bay.

Acknowledgements This study was funded by the National Natural Science Foundation of China (Grant Nos. 41071011 and 41271016), the Startup Foundation for Introducing Talent of Nangjing University of Information Science and Technology (No. 2016r053), and the National Basic Research Program of China (No. 2010CB951202). Prof. Zhijun Dai is thanked for the helpful suggestions.

References

Brown J M, Davies A G (2010). Flood/ebb tidal asymmetry in a shallow sandy estuary and the impact on net sand transport. Geomorphology, 114(3): 431–439

Chu Z X, Sun X G, Zhai S K., Xu K H (2006). Changing pattern of accretion/erosion of the modern Yellow River (Huanghe) subaerial delta, China: based on remote sensing images. Marine Geology, 227 (1–2): 13–30

Dai Z J, Du J Z, Zhang X L, Su N, Li J F (2011). Variation of riverine matrial loads and environmental consequences on the Changjiang (Yantze) estuary in recent decades (1955−2008). Environ Sci Technol, 45(1): 223–227

Dai Z J, Liu J T (2013). Impacts of large dams on downstream fluvial sedimentation: an example of the Three Gorges Dam (TGD) on the Changjiang (Yangtze River). J Hydrol (Amst), 480: 10–18

Dai Z J, Liu J T, Fu G, Xie H L (2013a). A thirteen-year record of bathymetric changes in the North Passage, Changjiang (Yangtze) Estuary. Geomorphology, 187: 101–107

Dai Z J, Liu J T, Xie H L, Shi W Y (2013b). Sedimentation in the Outer Hangzhou Bay, China: the influence of Changjing sediment load. J Coast Res, 30(6): 1218–1225

Eric M, Jacques D, Olivier C, Henri E, Xalbat C, Jon E, Eric V, Peggy R (1999). Assessment of suspended matter input into the oceans by small mountainous coastal rivers: the case of the Bay of Biscay. Comptes Rendus de l'Académie des Sciences – Series IIA – Earth and Planetary Science, 329(6): 413–420

Farnsworth K L, Milliman J D (2003). Effect of climatic and anthropogenic change on small mountainous rivers: the Salinas River example. Global and Planetary Change, 39(1–2): 53–64

Frihy O E, Debes E A, El Sayed W R (2003). Processes reshaping the Nile delta promontories of Egypt: pre and post – protection. Geomorphology, 53(3−4): 263–279

Gao S (1998). On the restoration and improvement of deteriorated coastal environments, with special reference to Yuehu Logoon, Shandong Peninsula, China. World Sci – tech. Res Dev, 20(4): 123–126 (in Chinese)

Gao S (2002). Water environment problems in development of tidal inlet systems. Water Resources Protection, 3: 18–21 (in Chinese)

Hamed K H, Rao A R (1998). A modified Mann – Kendall trend test for autocorrelated data. Journal of Hydrology, 204, (1–4): 182–196

Hao X M, Chen Y N, Xu C C, Li W (2008). Impacts of climate change and human activities on the Surface runoff in the Tarim River basin over the last fifty years. Water Resour Manage, 22(9): 1159–1171

Harish G, Shuh-Ji K, Minhan D (2012). The role of mega dams in reducing sediment fluxes: a case study of large Asian rivers. Journal of Hydrology, (464–465): 447–458

Kong D X, Miao C Y, Borthwick A G L, Duan Q Y, Liu H, Sun Q H, Ye A Z, Di Z H, Gong W (2015a). Evolution of the Yellow River Delta and its relationship with runoff and sediment load from 1983 to 2011. J Hydrol (Amst), 520: 157–167

Kong D X, Miao C Y, Wu J W, Jiang L, Duan Q Y (2015b). Bi-objective analysis of water-sediment regulation for channel scouring and delta maintenance: a study of the lower Yellow River. Global Planet Change, 133: 27–34

Li Q, Yu M, Lu G, Cai T, Bai X, Xia Z (2011). Impacts of the Gezhouba and Three Gorges reservoirs on the sediment regime in the Yangtze River, China. Journal of Hydrology, 403(3–4): 224–233

Li X Y, Luo Y, Wang L X (2003). Study on the disturbance of human activities on the hydrological process in Tarim River Watershed. Journal of Zhengzhou University(Engineering Science), 23: 93–98 (in Chinese)

Lu X X, Chen X Q (2008). Large Asian rivers and their interactions with estuaries and coasts. Quat Int, 186(1): 1–3

Miao C Y, Ni J R, Borthwick A G L (2010). Recent changes of water discharge and sediment load in the Yellow River basin, China. Prog Phys Geogr, 34(4): 541–561

Milliman J D, Syvitski J P M (1992). Geomorphic/tectonic control of sediment discharge to the ocean: the importance of small mountainous rivers. J Geol, 100(5): 525–544

Mohammad A G, Adam M A (2010). The impact of vegetative cover type on runoff and soil erosion under different land uses. Catena, 81 (2): 97–103

Oudin L, Andréassian V, Lerat J, Michel C (2008). Has land cover a significant impact on mean annual streamflow? An international assessment using 1508 catchments. Journal of hydrology, 357(3–4): 303–316

Prandle D (2003). Relationships between tidal dynamics and bathymetry in strongly convergent estuaries. J Phys Oceanogr, 33(12): 2738–2750

Ramos e Silva C A, Dávalos P B, da Silveira Lobo Sternberg L, Soares de Souza F E, Constantino Spyrides M H, Lucio P S (2010). The influence of shrimp farms organic waste management on chemical water quality. Estuar Coast Shelf Sci, 90(1): 55–60

Ryu J H, Kim C H, Lee Y K, Won J S, Chun S S, Lee S (2008). Detecting the intertidal morphologic change using satellite data. Estuar Coast Shelf Sci, 78(4): 623–632

Shandong Provincial Department of Land and Resources China (2007). Shandong Land Resources Atlas. Jinan: Shandong Cartographic Publishing House, 13 (in Chinese)

Sun G, Zhou G Y, Zhang Z Q, Wei X H, Steven G M, James M V (2006). Potential water yield reduction due to forestation across China. Journal of Hydrology, 328 (3–4): 548–558

Sun Q J, Lin Y Z, Wu Y L, Li S D, Jin R X (1987). Geography of Shandong Province. Beijing: China Education Press, 97 (in Chinese)

Syvitski J P M, Saito Y (2007). Morphodynamics of deltas under the influence of humans. Global Planet Change, 57(3−4): 261–282

Tian Q, Prange M, Merkel U (2016). Precipitation and temperature changes in the major Chinese river basins during 1957–2013 and links to sea surface temperature. Journal of Hydrology, 536: 208–221

Walling D E (2006). Human impact on land-ocean sediment transfer by the world's rivers. Geomorphology, 79(3–4): 192–216

Wang H, Bi N, Saito Y, Wang Y, Sun X, Zhang J, Yang Z (2010). Recent changes in sediment delivery by the Huanghe (Yellow River) to the sea: causes and environmental implications in its estuary. Journal of Hydrology, 391 (3–4): 302–313

Wang W H, ed. (1993). China Bay Records (the fourth volume). Beijing: China Ocean Press, 34–45 (in Chinese)

Water Resources Department of Shandong Province (1999). Registration data compilation of large and medium-sized reservoirs in Shandong Province, 17 (in Chinese)

Wu C S, Yang S L, Lei Y P (2012). Quantifying the anthropogenic and climatic impacts on water discharge and sediment load in the Pearl River (Zhujiang), China (1954–2009). Journal of Hydrology, (452–453): 190–204

Xia D X, Liu Z X (1990). Classification of bays in China. Oceanol Limnol Sin, 21(2): 185–191 (in Chinese)

Xie B, Ding Z, Wang X (2004). Impact of the intensive shrimp farming on the water quality of the adjacent coastal creeks from Eastern China. Marine Pollution Bulletin, 48 (5–6): 543–553

Xie B, Yu K (2007). Shrimp farming in China: operating characteristics, environmental impact and perspectives. Ocean Coast Manage, 50(7): 538–550

Xu J X (2001). The Yellow River mouth extension since 1194 as influenced by human activities. Progress in Geography, 20: 1–9

Xu J X, Sun J (2007). Sediment yield in major sediment source areas of the Upper Changjiang River Basin in response to human activities. Scientia Geographica Sinica, 27(2): 211–218

Xu K H, John D M, Xu H (2010). Temporal trend of precipitation and runoff in major Chinese Rivers since 1951. Journal of Hydrology, 73 (3–4): 219–232

Yang S L, Li M, Dai S B, Liu Z, Zhang J, Ding P X (2006). Drastic decrease in sediment supply from the Yangtze River and its challenge to coastal wetland management. Geophys Res Lett, 33(6): L06408

Yang S L, Milliman J D, Li P, Xu K H (2011). 50000 dams later: erosion of the Yangtze River and its delta. Global Planet Change, 75(1−2): 14–20

Yang S L, Zhang J, Zhu J , Smith J P , Dai S B , Gao A , Li P (2005). Impact of dams on Yangtze River sediment supply to the sea and delta intertidal wetland response. J Geophys Res, 110, F03006

Zhao B, Guo H, Yan Y, Wang Q, Li B (2008). A simple waterline approach for tidelands using multi-temporal satellite images: a case study in the Yangtze Delta. Estuar Coast Shelf Sci, 77(1): 134–142